

Enabling Digital Twin in Vehicular Edge Computing: A Multi-Agent Multi-Objective Deep Reinforcement Learning Solution

Xincao Xu, Kai Liu, *Senior Member, IEEE*, Penglin Dai, *Member, IEEE*, and Biwen Chen

Abstract—With recent advances in sensing technologies, wireless communications, and computing paradigms, traditional vehicles are evolving to electronic consumer products, driving the research on digital twins in vehicular edge computing (DT-VEC). This paper makes the first attempt to achieve the quality-cost tradeoff in DT-VEC. First, a DT-VEC architecture is presented, where the heterogeneous information can be sensed by vehicles and uploaded to the edge node via vehicle-to-infrastructure (V2I) communications. The DT-VEC are modeled at the edge node, forming a logical view to reflect the physical vehicular environment. Second, we model the DT-VEC by deriving an ISAC (integrated sensing and communication)-assisted sensing model and a reliability-guaranteed uploading model. Third, we define the quality of DT-VEC by considering the timeliness and consistency, and define the cost of DT-VEC by considering the redundancy, sensing cost, and transmission cost. Then, a bi-objective problem is formulated to maximize the quality and minimize the cost. Fourth, we propose a multi-agent multi-objective (MAMO) deep reinforcement learning solution implemented distributedly in the vehicles and the edge nodes. Specifically, a dueling critic network is proposed to evaluate the advantage of action over the average of random actions. Finally, we give a comprehensive performance evaluation, demonstrating the superiority of the proposed MAMO.

Index Terms—Digital twin, vehicular edge computing, deep reinforcement learning, integrated sensing and communication

I. INTRODUCTION

RECENT advances in sensing technologies, wireless communications, and computing paradigms drive the development of modern new-energy and intelligent vehicles, which represent typical electronic consumer products. Various on-board sensors are equipped by modern vehicles to enhance the environment-sensing ability [1]. On the other hand, integrated sensing and communication (ISAC) [2] has emerged as a key technology for sensing and communication in the 5G era, in which cellular vehicle-to-everything (C-V2X) [3] is the critical enabler for vehicular communications. Meanwhile, vehicular edge computing (VEC) [4] is a potential paradigm for enabling computation-intensive and latency-critical applications at the edge of vehicular networks. These advances become strong driving forces of developing digital twins (DTs) [5] in vehicular networks, which are the virtual representations of

physical entities, such as vehicles, pedestrians, and roadside infrastructures.

Recently, ISAC has attracted much attention in vehicular networks. The information-theoretic limits of ISAC are discussed in [6]. Some researchers focus on the development of ISAC systems in vehicular networks, such as the 5G new radio (NR) frame structure based ISAC system [7], and orthogonal time frequency space signals based ISAC system [8]. On the other hand, great efforts have been devoted to vehicular data dissemination, such as end-edge-cloud cooperative data dissemination architecture [9] and intent-based network control framework [10]. To improve caching efficiency, some other researchers proposed vehicular content caching frameworks, such as blockchain-empowered content caching [11], cooperative coding and caching scheduling [12], and edge-cooperative content caching [13]. Some researchers studied vehicular task offloading mechanisms, such as deep-learning-based energy-efficient task offloading [14], real-time multi-period task offloading [15], alternating direction method of multipliers (ADMMs) and particle swarm optimization (PSO) combined task offloading [16]. These studies formed the basis for investigating DTs in vehicular networks with respect to data dissemination, information caching, and task offloading technologies.

Several studies have been studied on detecting technologies in intelligent transportation systems (ITSs) [17], such as rain-drop quantity detection [18] and driver fatigue detection [19]. Some researchers studied predicting technologies for vehicle status, such as hybrid velocity-profile prediction [20] and acceleration prediction [21]. Some other researchers developed scheduling schemes in vehicular networks, such as physical-ratio-K interference model-based broadcast scheduling [22] and established map model-based path planning [23]. In addition, some studies proposed controlling algorithms for intelligent vehicles, such as vehicle acceleration controlling [24] and electric vehicle (EV) charging scheduling [25]. These technologies facilitated the implementation of various ITSs regarding to detecting, predicting, scheduling, and controlling technologies. A few studies have concerned the information quality in vehicular networks, including timeliness [26], [27] and accuracy [28], [29]. Nevertheless, to the best of our knowledge, none of the previous studies have investigated the quality-cost tradeoff of digital twins in vehicular edge computing (DT-VEC).

In this paper, we put the first efforts on realizing high-quality and low-cost DT-VEC by addressing the following

arXiv:2210.17386v1 [cs.NI] 31 Oct 2022

Manuscript received. (Corresponding author: Biwen Chen)

Xincao Xu, Kai Liu, and Biwen Chen are with the College of Computer Science, Chongqing University, Chongqing 400040, China. (e-mail: near, liukai0807, macrochen@cqu.edu.cn).

Penglin Dai is with the School of Computing and Artificial Intelligence, Southwest Jiaotong University, Chengdu 611756, China. (e-mail: penglindai@swjtu.edu.cn).

critical issues. First, the physical information is naturally highly dynamic in vehicular networks, which requires real-time sensing and updating. It is crucial to evaluate the interrelationship between sensing frequency, queuing delay, and transmission delay to guarantee information freshness. Second, the sensed information may be duplicated in the temporal or spatial domain. Thus, vehicles with different sensing capacities are expected to be cooperated in a distributed way to enhance the utilization of communication and computing resources. Third, the physical information is heterogeneous regarding to distribution, updating frequency, and modality, which poses significant difficulties in modeling the DT-VEC. Fourth, vehicles and edge nodes have limited communication resources. In addition, high-frequency sensing may lead to extra sensing and uploading workloads. Thus, edge nodes need to construct DT-VEC at a lower cost. To sum up, realizing the high-quality and low-cost DT-VEC is crucial yet challenging.

The primary contributions of this paper are summarized as follows.

- We present a DT-VEC architecture consisting of intelligent vehicles with sensing and communication capabilities and the edge node, where DT-VEC are modeled via information fusion. The heterogeneous information can be sensed via either ISAC or onboard sensors, which are queued in vehicles for uploading via vehicle-to-infrastructure (V2I) communications. Then, a logical view is constructed based on DT-VEC. A high-quality view can reflect the physical vehicular environment accurately and timely but may cost more communication and computing resources.
- We derive the DT-VEC model by giving the formal definition. To capture the information characteristics, we derive an ISAC-assisted sensing model based on multi-class M/G/1 priority queue, in which the queuing times of information with different frequencies are obtained. On the other hand, the reliability-guaranteed uploading model is derived, in which the successful transmission probability is obtained based on channel fading distribution and signal-to-noise ratio (SNR) threshold.
- We formulate the bi-objective problem to maximize the system quality and minimize the system cost, simultaneously. In particular, we define the quality of DT-VEC by considering the timeliness and consistence, and define the cost of DT-VEC by considering redundancy, sensing cost, and transmission cost. On this basis, we further design two metrics, namely, system quality and system cost, and present the bi-objective problem, aiming at maximizing the system quality and minimizing the system cost, simultaneously.
- We propose a multi-agent multi-objective (MAMO) deep reinforcement learning solution, which is implemented distributedly in vehicles and the edge node. The action space of each vehicle consists of the sensing information decision, sensing frequency, uploading priority, and transmission power allocations. The action space of each edge node is the V2I bandwidth allocation. In particular, a dueling critic network is utilized to output Q values by

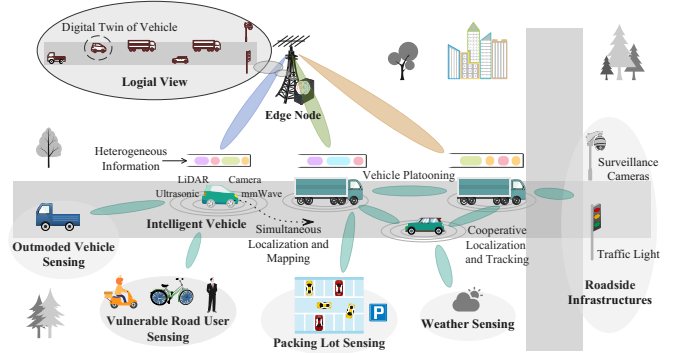


Fig. 1. Digital twin model in vehicular edge computing

evaluating the advantage of action over the average of random actions.

The rest of this paper is organized as follows. Section II presents the system architecture. Section III presents the system model. Section IV formulates the problem. Section V proposes the solution. Section VI evaluates the performance. Finally, Section VII concludes this paper.

II. SYSTEM ARCHITECTURE

In this section, we present the DT-VEC architecture shown in Fig. 1. Intelligent vehicles are equipped with various onboard sensors, such as ultrasonic sensors, light detection and ranging (LiDAR), optical cameras, and millimeter wave (mmWave) radars. The heterogeneous information, including vehicle status, vulnerable road user status, packing lot status, weather condition, and roadside infrastructure status, are collaboratively sensed by vehicles via onboard sensors and ISAC (e.g., the outmoded vehicles without sensing and communication abilities can be sensed by intelligent vehicles via V2I communications). In particular, the information is queued in vehicles for uploading via the V2I bandwidth allocated by the corresponding edge nodes, such as 5G base stations and roadside units (RSUs). Such information can be used to model the DT-VEC via artificial intelligence (AI) and machine learning (ML) methods and further construct the logical view of the physical vehicular environment. Logical views are essential for the quality of service (QoS) of up-layer vehicular applications in ITSs, such as simultaneous localization and mapping (SLAM), vehicle platooning, and cooperative localization and tracking. A high-quality view can reflect the physical vehicular environment accurately and timely. Nevertheless, it may require more frequent or redundant sensing and uploading, which increases the additional overheads on energy consumption and information processing.

The system characteristics are summarized as follows. First, the heterogeneous information is sensed by vehicles at different sensing frequencies. Therefore, the arrival times of various pieces of information may be different. In addition, increasing the sensing frequency may improve the timeliness of information, but it also prolongs the queuing latency. Second, it is essential to determine the uploading priority by considering the different data sizes of information, V2I communication

connectivity, and DT-VEC requirements. Third, due to the restricted communication resources of vehicles and edge nodes, including vehicle transmission power and edge bandwidth, it may not be sufficient to support the data uploading timely with acceptable cost. It is meaningful to allocate communication resources efficiently and economically to improve resource utilization. As illustrated above, it is critical yet challenging to model high-quality and low-cost DT-VEC.

III. SYSTEM MODEL

A. Notations

The set of discrete time slots is denoted by $\mathbf{T} = \{1, 2, \dots, t, \dots, T\}$, where T is the number of time slots. Let \mathbf{D} denote the set of heterogeneous information. Each information $d \in \mathbf{D}$ is characterized by a three-tuple $d = (\text{type}_d, u_d, |d|)$, where type_d , u_d , and $|d|$ are the type, updating interval, and data size, respectively. We denote \mathbf{S} as the set of vehicles. Each vehicle $s \in \mathbf{S}$ is characterized by a three-tuple $s = (l_s^t, \mathbf{D}_s, \pi_s)$, where l_s^t , \mathbf{D}_s , and π_s are the location, sensed information set, and transmission power, respectively. For each information $d \in \mathbf{D}_s$, the sensing cost (i.e., energy consumption) in vehicle s is denoted by $\phi_{d,s}$. Let \mathbf{E} denote the set of edge nodes. Each edge node $e \in \mathbf{E}$ is characterized by a three-tuple $e = (l_e, r_e, b_e)$, where l_e , r_e , and b_e are the location, communication range, and bandwidth, respectively. The distance between vehicle s and edge node e is denoted by $\text{dis}_{s,e}^t \triangleq \text{distance}(l_s^t, l_e), \forall s \in \mathbf{S}, \forall e \in \mathbf{E}, \forall t \in \mathbf{T}$, where $\text{distance}(\cdot, \cdot)$ is the Euclidean distance. The set of vehicles within the radio coverage of edge node e at time t is denoted by $\mathbf{S}_e^t = \{s \mid \text{dis}_{s,e}^t \leq r_e, \forall s \in \mathbf{S}\}, \mathbf{S}_e^t \subseteq \mathbf{S}$.

The sensing information indicator, indicating whether information d is sensed by vehicle s at time t , is denoted by

$$c_{d,s}^t \in \{0, 1\}, \forall d \in \mathbf{D}_s, \forall s \in \mathbf{S}, \forall t \in \mathbf{T} \quad (1)$$

Thus, the set of information sensed by vehicle s at time t is denoted by $\mathbf{D}_s^t = \{d \mid c_{d,s}^t = 1, \forall d \in \mathbf{D}_s\}, \mathbf{D}_s^t \subseteq \mathbf{D}_s$. The information types are distinct for any information $d \in \mathbf{D}_s^t$, i.e., $\text{type}_{d^*} \neq \text{type}_d, \forall d^* \in \mathbf{D}_s^t \setminus \{d\}, \forall d \in \mathbf{D}_s^t$. The sensing frequency of information d in vehicle s at time t is denoted by $\lambda_{d,s}^t$. The sensing frequencies of information d in vehicle s at time t should meet the requirement of its sensing ability.

$$\lambda_{d,s}^t \in [\lambda_{d,s}^{\min}, \lambda_{d,s}^{\max}], \forall d \in \mathbf{D}_s^t, \forall s \in \mathbf{S}, \forall t \in \mathbf{T} \quad (2)$$

where $\lambda_{d,s}^{\min}$ and $\lambda_{d,s}^{\max}$ are the minimum and maximum of sensing frequency for information with type_d in vehicle s , respectively. The uploading priority of information d in vehicle s at time t is denoted by $p_{d,s}^t$, and we have

$$p_{d^*,s}^t \neq p_{d,s}^t, \forall d^* \in \mathbf{D}_s^t \setminus \{d\}, \forall d \in \mathbf{D}_s^t, \forall s \in \mathbf{S}, \forall t \in \mathbf{T} \quad (3)$$

The transmission power of vehicle s at time t is denoted by π_s^t , and it can not exceed the power capacity of vehicle s , i.e.,

$$\pi_s^t \in [0, \pi_s], \forall s \in \mathbf{S}, \forall t \in \mathbf{T} \quad (4)$$

The V2I bandwidth allocated by edge node e for vehicle s at time t is denoted by $b_{s,e}^t$, and we have

$$b_{s,e}^t \in [0, b_e], \forall s \in \mathbf{S}_e^t, \forall e \in \mathbf{E}, \forall t \in \mathbf{T} \quad (5)$$

The sum of V2I bandwidth allocated by edge node e cannot exceed its capacity b_e , i.e., $\sum_{\forall s \in \mathbf{S}_e^t} b_{s,e}^t \leq b_e, \forall t \in \mathbf{T}$. The primary notations are summarized in Table I.

TABLE I
SUMMARY OF PRIMARY NOTATIONS

Notations	Descriptions
\mathbf{T}, \mathbf{D}	Set of discrete time slots, Set of heterogeneous information
\mathbf{S}, \mathbf{E}	Set of vehicles, Set of edge nodes
type_d	Type of information d
u_d	Updating interval of information d
l_s^t	Location of vehicle s at time t
\mathbf{D}_s	Set of information sensed by vehicle s
π_s	Transmission power of vehicle s
l_e	Location of edge node e
r_e	Communication range of edge node e
b_e	Bandwidth capacity of edge node e
$\text{dis}_{s,e}^t$	Distance between vehicle s and edge node e at time t
\mathbf{S}_e^t	Set of vehicles within the coverage of edge node e
\mathbf{V}'	Set of physical entities in vehicular edge computing
\mathbf{V}	Set of digital twins in vehicular edge computing (DT-VEC)
$y_{d,v}$	Binary indicates whether information d is required by DT-VEC v
$\mathbf{D}_{v'}$	Set of information associated with physical entity v'
\mathbf{V}_e^t	Set of DT-VEC in edge node e at time t
$\mathbf{D}_{v,e}^t$	Set of information received by edge node e and required by DT-VEC v
$c_{d,s}^t$	Binary indicates whether information d is sensed by vehicle s
\mathbf{D}_s^t	Set of information sensed by vehicle s at time t
$\lambda_{d,s}^t$	Sensing frequency of information d in vehicle s at time t
$p_{d,s}^t$	Uploading priority of information d in vehicle s at time t
π_s^t	Transmission power of vehicle s at time t
$b_{s,e}^t$	Bandwidth allocated by edge node e for vehicle s at time t
$a_{d,s}^t$	Arrival moment of the information with type_d in vehicle s
$u_{d,s}^t$	Updating moment of the information with type_d in vehicle s
$\mathbf{D}_{d,s}^t$	Set of information with higher uploading priority than d
$q_{d,s}^t$	Queuing time of information d in vehicle s
$g_{d,s,e}^t$	Transmission time of information d
$\mathbf{D}_{s,e}^t$	Set of information transmitted by vehicle s and received at e

B. DT-VEC Model

Denote the set of physical entities as \mathbf{V}' in VEC. For each entity $v' \in \mathbf{V}'$, there is a digital twin modeled in the edge node. We denote the set of DT-VEC as \mathbf{V} , and we give the formal definition of the digital twin in vehicular edge computing as follows.

Definition 1 (*Digital twin in vehicular edge computing, DT-VEC*). The DT-VEC v is the information organism about physical entity v' in VEC, such as vehicles, pedestrians, and roadside infrastructures.

$$v \triangleq f(\mathbf{D}_{v'}) \cong v', \exists v \in \mathbf{V}, \forall v' \in \mathbf{V}' \quad (6)$$

where $f: \mathbf{V}' \rightarrow \mathbf{V}$ is a bijection function generated by AI/ML methods based on edge intelligence provided by the edge node. $\mathbf{D}_{v'}$ is the set of information associated with entity v' , and can be represented by $\mathbf{D}_{v'} = \{d \mid y_{d,v'} = 1, \forall d \in \mathbf{D}\}, \forall v' \in \mathbf{V}'$, where $y_{d,v'}$ is a binary indicating whether information d is associated by entity v' .

The size of $\mathbf{D}_{v'}$ is denoted by $|\mathbf{D}_{v'}|$. Each entity may require multiple pieces of information, i.e., $|\mathbf{D}_{v'}| = \sum_{\forall d \in \mathbf{D}} y_{d,v'} \geq$

1, $\forall v' \in \mathbf{V}'$. The set of DT-VEC in edge node e at time t is denoted by \mathbf{V}_e^t . Therefore, the set of information received by edge node e and required by DT-VEC v can be represented by $\mathbf{D}_{v,e}^t = \bigcup_{\forall s \in \mathbf{S}} (\mathbf{D}_{v'} \cap \mathbf{D}_{s,e}^t)$, $\forall v \in \mathbf{V}_e^t, \forall e \in \mathbf{E}$, and $|\mathbf{D}_{v,e}^t|$ is the number of information received by edge node e and required by DT-VEC v , which is computed by $|\mathbf{D}_{v,e}^t| = \sum_{\forall s \in \mathbf{S}} \sum_{\forall d \in \mathbf{D}_s} c_{d,s}^t y_{d,v'}$. To evaluate the DT-VEC, we further obtain the information characteristics, including arrival moment, updating moment, queuing time, and transmission time by deriving the ISAC-assisted sensing model and reliability-guaranteed uploading model.

C. ISAC-Assisted Sensing Model

In this section, we model ISAC-assisted sensing based on multi-class M/G/1 priority queue [30]. We assume that the uploading time distribution of information with type $_d$ in vehicle s stays stable within each time slot. The uploading time $\hat{g}_{d,s,e}^t$ of information with type $_d$ follows a class of General distribution with mean $\alpha_{d,s}^t$ and variance $\beta_{d,s}^t$. Therefore, the uploading workload ρ_s^t in vehicle s is represented by $\rho_s^t = \sum_{\forall d \in \mathbf{D}_s} \lambda_{d,s}^t \alpha_{d,s}^t$. According to the principle of multi-class M/G/1 priority queue, it requires $\rho_s^t < 1$ to guarantee the existence of the queue steady-state. The arrival moment of the freshest information with type $_d$ before time t is denoted by $a_{d,s}^t$, which is computed by

$$a_{d,s}^t = 1/\lambda_{d,s}^t [t\lambda_{d,s}^t] + i_{d,s}^t/2 \quad (7)$$

where $i_{d,s}^t$ is the transmission time of ISAC sensing signal, and $i_{d,s}^t = 0$ if the information is sensed by onboard sensors. The updating moment of the freshest information with type $_d$ before time t is denoted by $u_{d,s}^t$, which is computed by

$$u_{d,s}^t = \lfloor a_{d,s}^t/u_d \rfloor u_d \quad (8)$$

where u_d is the updating interval of information d .

The set of information with a higher uploading priority than information d is denoted by $\mathbf{D}_{d,s}^t$ and can be represented by $\mathbf{D}_{d,s}^t = \{d^* \mid p_{d^*,s}^t > p_{d,s}^t, \forall d^* \in \mathbf{D}_s^t\}$. Thus, the uploading workload ahead of information d in vehicle s at time t is denoted by

$$\rho_{d,s}^t = \sum_{\forall d^* \in \mathbf{D}_{d,s}^t} \lambda_{d^*,s}^t \alpha_{d^*,s}^t \quad (9)$$

According to the Pollaczek-Khintchine formula [31], the queuing time of information d in vehicle s is calculated by

$$q_{d,s}^t = \frac{1}{1 - \rho_{d,s}^t} \left[\alpha_{d,s}^t + \frac{\lambda_{d,s}^t \beta_{d,s}^t + \sum_{\forall d^* \in \mathbf{D}_{d,s}^t} \lambda_{d^*,s}^t \beta_{d^*,s}^t}{2(1 - \rho_{d,s}^t - \lambda_{d,s}^t \alpha_{d,s}^t)} \right] - \alpha_{d,s}^t \quad (10)$$

D. Reliability-Guaranteed Uploading Model

In this section, we model the reliability-guaranteed uploading based on channel fading distribution and SNR threshold. The SNR of V2I communications between vehicle s and edge node e at time t is denoted by [32]

$$\text{SNR}_{s,e}^t = \frac{1}{N_0} |h_{s,e}|^2 \tau \text{dis}_{s,e}^t - \varphi \pi_s^t \quad (11)$$

where N_0 is the additive white Gaussian noise (AWGN); $h_{s,e}$ is the channel fading gain; τ is a constant that depends on the antennas design, and φ is the path loss exponent. We assume that $|h_{s,e}|^2$ follows a class of distribution with the mean $\mu_{s,e}$ and variance $\sigma_{s,e}$, and the distribution set is represented by

$$\tilde{p} = \left\{ \mathbb{P} : \mathbb{E}_{\mathbb{P}} [|h_{s,e}|^2] = \mu_{s,e}, \mathbb{E}_{\mathbb{P}} [|h_{s,e}|^2 - \mu_{s,e}]^2 = \sigma_{s,e} \right\} \quad (12)$$

The transmission reliability is measured by the possibility that a successful transmission probability is beyond a reliability threshold.

$$\inf_{\mathbb{P} \in \tilde{p}} \Pr_{[\mathbb{P}]} (\text{SNR}_{s,e}^t \geq \text{SNR}_{s,e}^{\text{tgt}}) \geq \delta \quad (13)$$

where $\text{SNR}_{s,e}^{\text{tgt}}$ and δ are the target SNR threshold and reliability threshold, respectively. The set of information uploaded by vehicle s and received by edge node e is denoted by $\mathbf{D}_{s,e}^t = \bigcup_{\forall s \in \mathbf{S}_e} \mathbf{D}_s^t$.

According to the Shannon theory, the achievable transmission rate of V2I communications between vehicle s and edge node e at time t is denoted by $z_{s,e}^t$, which is computed by

$$z_{s,e}^t = b_s^t \log_2 (1 + \text{SNR}_{s,e}^t) \quad (14)$$

Thus, the transmission time of information d from vehicle s to edge node e , denoted by $g_{d,s,e}^t$, is computed by

$$g_{d,s,e}^t = \inf_{j \in \mathbb{R}^+} \left\{ \int_{k_{d,s}^t}^{k_{d,s}^t + j} z_{s,e}^t dt \geq |d| \right\} - k_{d,s}^t \quad (15)$$

where $k_{d,s}^t = t + q_{d,s}^t$ is the moment when vehicle s starts to transmit information d .

IV. PROBLEM FORMULATION

A. Quality of DT-VEC

First, the DT-VEC is modeled based on the continuously uploaded and time-varying information so that the information freshness is essential for the quality of DT-VEC.

Definition 2 (Timeliness of information d). The timeliness $\theta_{d,s} \in \mathbb{Q}^+$ of information d in vehicle s is defined as the duration between the updating and receiving moment of the information d .

$$\theta_{d,s} = a_{d,s}^t + q_{d,s}^t + g_{d,s,e}^t - u_{d,s}^t, \forall d \in \mathbf{D}_s^t, \forall s \in \mathbf{S} \quad (16)$$

Definition 3 (Timeliness of DT-VEC v). The timeliness $\Theta_v \in \mathbb{Q}^+$ of DT-VEC v is defined as the sum of the maximum timeliness of information associated with physical entity v' .

$$\Theta_v = \sum_{\forall s \in \mathbf{S}_e^t} \max_{\forall d \in \mathbf{D}_{v'} \cap \mathbf{D}_s^t} \theta_{d,s}, \forall v \in \mathbf{V}_e^t, \forall e \in \mathbf{E} \quad (17)$$

Second, since different types of information have their sensing frequencies and uploading priorities, keeping the versions of different types of information associated with the same physical entity as close as possible is important.

Definition 4 (*Consistency of DT-VEC v*). The consistency $\Psi_v \in \mathbb{Q}^+$ of DT-VEC v is defined as the maximum of the difference between information updating time.

$$\Psi_v = \max_{\forall d \in \mathbf{D}_{v,e}^t, \forall s \in \mathbf{S}_e^t} u_{d,s}^t - \min_{\forall d \in \mathbf{D}_{v,e}^t, \forall s \in \mathbf{S}_e^t} u_{d,s}^t, \forall v \in \mathbf{V}_e^t, \forall e \in \mathbf{E} \quad (18)$$

Finally, we give the formal definition of the quality of DT-VEC, synthesizing the timeliness and consistency of DT-VEC.

Definition 5 (*Quality of DT-VEC, QDT*). The quality of DT-VEC $\text{QDT}_v \in (0, 1)$ is defined as a weighted average of normalized timeliness and normalized consistency of DT-VEC v .

$$\text{QDT}_v = w_1 \hat{\Theta}_v + w_2 \hat{\Psi}_v, \forall v \in \mathbf{V}_e^t, \forall e \in \mathbf{E} \quad (19)$$

where $\hat{\Theta}_v \in (0, 1)$ and $\hat{\Psi}_v \in (0, 1)$ denote the normalized timeliness and normalized consistency, respectively, which can be obtained by rescaling the range of the timeliness and consistency in $(0, 1)$ via the min-max normalization. The weighting factors for $\hat{\Theta}_v$ and $\hat{\Psi}_v$ are denoted by w_1 and w_2 , respectively, and we have $w_1 + w_2 = 1$. The weighting factors can be tuned accordingly based on the different requirements of upper-layer applications.

B. Cost of DT-VEC

First, vehicles may sense the same information redundantly, which may cost more resources.

Definition 6 (*Redundancy of information d*). The redundancy $\xi_d \in \mathbb{N}$ of information d is defined as the number of information with type d .

$$\xi_d = |\mathbf{D}_{d,v,e}| - 1, \forall d \in \mathbf{D}_v, \forall v \in \mathbf{V}_e^t, \forall e \in \mathbf{E} \quad (20)$$

where $\mathbf{D}_{d,v,e}$ is the set of the information received by edge node e and required by DT-VEC v with type d , which is represented by $\mathbf{D}_{d,v,e} = \{d^* | \text{type}_{d^*} = \text{type}_d, \forall d^* \in \mathbf{D}_{v,e}^t\}$, $\forall d \in \mathbf{D}_{v,e}^t$.

Definition 7 (*Redundancy of DT-VEC v*). The redundancy $\Xi_v \in \mathbb{N}$ of DT-VEC v is defined as the sum of redundancy of information in DT-VEC v .

$$\Xi_v = \sum_{\forall d \in \mathbf{D}_v} \xi_d, \forall v \in \mathbf{V}_e^t, \forall e \in \mathbf{E} \quad (21)$$

Definition 8 (*Sensing cost of DT-VEC v*). The sensing cost $\Phi_v \in \mathbb{Q}^+$ of DT-VEC v is defined as the sum of information sensing cost of information required by DT-VEC v .

$$\Phi_v = \sum_{\forall s \in \mathbf{S}_e^t} \sum_{\forall d \in \mathbf{D}_{v'} \cap \mathbf{D}_s^t} \phi_{d,s}, \forall v \in \mathbf{V}_e^t, \forall e \in \mathbf{E} \quad (22)$$

Second, information transmission requires energy consumption of vehicles, i.e., the transmission power consumption.

Definition 9 (*Transmission cost of information d*). The transmission cost $\omega_{d,s} \in \mathbb{Q}^+$ of information d in vehicle s is defined as the consumed transmission power during the information uploading.

$$\omega_{d,s} = \pi_s^t g_{d,s,e}^t, \forall d \in \mathbf{D}_s^t \quad (23)$$

Definition 10 (*Transmission cost of DT-VEC v*). The transmission cost $\Omega_v \in \mathbb{Q}^+$ of DT-VEC v is defined as the sum of information sensing cost in DT-VEC v .

$$\Omega_v = \sum_{\forall s \in \mathbf{S}_e^t} \sum_{\forall d \in \mathbf{D}_{v'} \cap \mathbf{D}_s^t} \omega_{d,s}, \forall v \in \mathbf{V}_e^t, \forall e \in \mathbf{E} \quad (24)$$

Finally, we give the formal definition of the cost of the DT-VEC, synthesizing the redundancy, sensing cost, and transmission cost.

Definition 11 (*Cost of DT-VEC, CDT*). The cost of DT-VEC $\text{CDT}_v \in (0, 1)$ is defined as a weighted average of normalized redundancy, normalized sensing cost, and normalized transmission cost of DT-VEC v .

$$\text{CDT}_v = w_3 \hat{\Xi}_v + w_4 \hat{\Phi}_v + w_5 \hat{\Omega}_v, \forall v \in \mathbf{V}_e^t, \forall e \in \mathbf{E} \quad (25)$$

where $\hat{\Xi}_v \in (0, 1)$, $\hat{\Phi}_v \in (0, 1)$, and $\hat{\Omega}_v \in (0, 1)$ denote the normalized redundancy, normalized sensing cost, and normalized transmission cost of DT-VEC v , respectively. The weighting factors for $\hat{\Xi}_v$, $\hat{\Phi}_v$, and $\hat{\Omega}_v$ are denoted by w_3 , w_4 , and w_5 , respectively. Similarly, we have $w_3 + w_4 + w_5 = 1$.

C. Bi-Objective Problem

On the basis of the QDT/CDT definition, we define the system quality and system cost as follows.

Definition 12 (*System quality*). The system quality $\mathcal{Q} \in (0, 1)$ is defined as the average of the complement of QDT for each DT-VEC in edge nodes during the scheduling period \mathbf{T} .

$$\mathcal{Q} = \frac{\sum_{\forall t \in \mathbf{T}} \sum_{\forall e \in \mathbf{E}} \sum_{\forall v \in \mathbf{V}_e^t} (1 - \text{QDT}_v)}{\sum_{\forall t \in \mathbf{T}} \sum_{\forall e \in \mathbf{E}} |\mathbf{V}_e^t|} \quad (26)$$

Definition 13 (*System cost*). The system cost $\mathcal{C} \in (0, 1)$ is defined as the average of CDT for each DT-VEC in edge nodes during the scheduling period \mathbf{T} .

$$\mathcal{C} = \frac{\sum_{\forall t \in \mathbf{T}} \sum_{\forall e \in \mathbf{E}} \sum_{\forall v \in \mathbf{V}_e^t} \text{CDT}_v}{\sum_{\forall t \in \mathbf{T}} \sum_{\forall e \in \mathbf{E}} |\mathbf{V}_e^t|} \quad (27)$$

Given a solution $x = (\mathbf{C}, \mathbf{\Lambda}, \mathbf{P}, \mathbf{\Pi}, \mathbf{B})$, where \mathbf{C} denotes the determined sensing information, $\mathbf{\Lambda}$ denotes the determined sensing frequencies, \mathbf{P} denotes the determined uploading priorities, $\mathbf{\Pi}$ denotes the determined transmission power, and \mathbf{B} denotes the determined V2I bandwidth allocation,

$$\begin{cases} \mathbf{C} &= \{c_{d,s}^t | \forall d \in \mathbf{D}_s, \forall s \in \mathbf{S}, \forall t \in \mathbf{T}\} \\ \mathbf{\Lambda} &= \{\lambda_{d,s}^t | \forall d \in \mathbf{D}_s^t, \forall s \in \mathbf{S}, \forall t \in \mathbf{T}\} \\ \mathbf{P} &= \{p_{d,s}^t | \forall d \in \mathbf{D}_s^t, \forall s \in \mathbf{S}, \forall t \in \mathbf{T}\} \\ \mathbf{\Pi} &= \{\pi_s^t | \forall s \in \mathbf{S}, \forall t \in \mathbf{T}\} \\ \mathbf{B} &= \{b_s^t | \forall s \in \mathbf{S}, \forall t \in \mathbf{T}\} \end{cases} \quad (28)$$

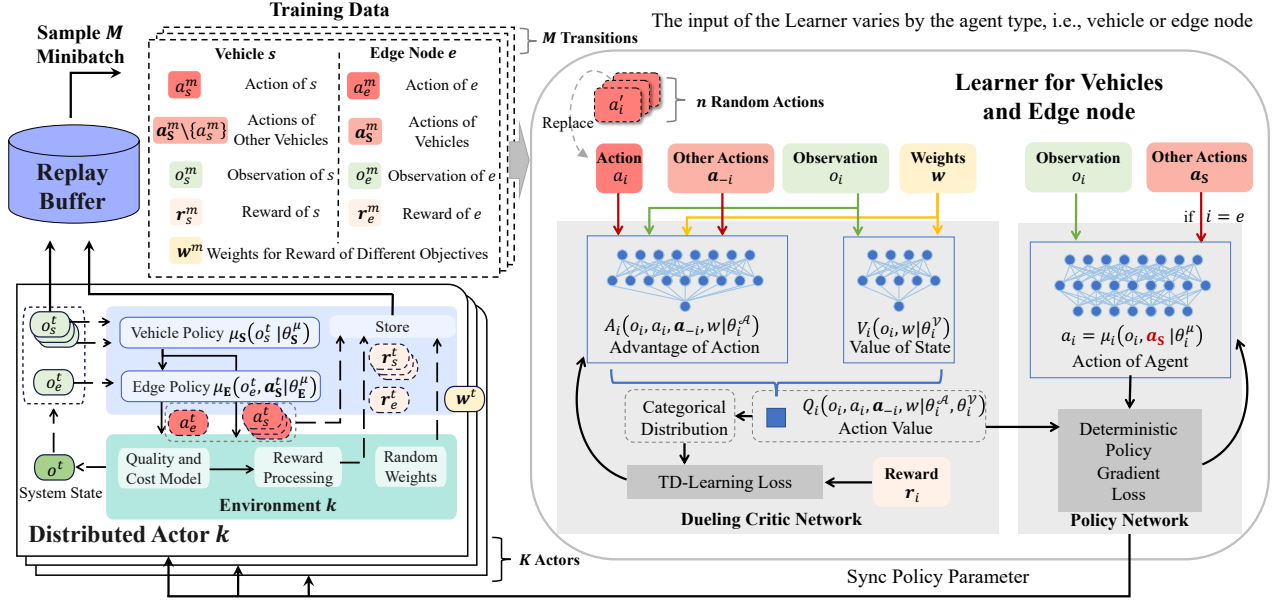


Fig. 2. Multi-agent multi-objective deep reinforcement learning model

we formulate the bi-objective problem aiming at maximizing the system quality and minimizing the system cost simultaneously, which is expressed by

$$\begin{aligned}
 \mathbf{P1} : & \max \mathcal{Q}, \min \mathcal{C} \\
 \text{s.t.} & (1) \sim (5) \\
 \text{C1} : & \sum_{\forall d \subseteq \mathbf{D}_s^t} \lambda_{d,s}^t \mu_d < 1, \forall s \in \mathbf{S}, \forall t \in \mathbf{T} \\
 \text{C2} : & \inf_{\mathbb{P} \in \tilde{\mathcal{P}}} \Pr_{[\mathbb{P}]} (\text{SNR}_{s,e}^t \geq \text{SNR}_{s,e}^{\text{tgt}}) \geq \delta, \forall s \in \mathbf{S}, \forall t \in \mathbf{T} \\
 \text{C3} : & \sum_{\forall s \in \mathbf{S}_e^t} b_s^t \leq b_e, \forall t \in \mathbf{T}
 \end{aligned} \tag{29}$$

where C1 guarantees the queue steady-state and C2 guarantees the transmission reliability. C3 requires that the sum of V2I bandwidth allocated by the edge node e cannot exceed its capacity b_e . According to the definition of system cost, we define the system profit as follows.

Definition 14 (System profit). The system profit $\mathcal{P} \in (0, 1)$ is defined as the average of the complement of CDT for each DT-VEC in edge nodes during the scheduling period \mathbf{T} .

$$\mathcal{P} = \frac{\sum_{\forall t \in \mathbf{T}} \sum_{\forall e \in \mathbf{E}} \sum_{\forall v \in \mathbf{V}_e^t} (1 - \text{CDT}_v)}{\sum_{\forall t \in \mathbf{T}} \sum_{\forall e \in \mathbf{E}} |\mathbf{V}_e^t|} \tag{30}$$

Thus, the problem $\mathbf{P1}$ can be rewritten as follows.

$$\begin{aligned}
 \mathbf{P2} : & \max (\mathcal{Q}, \mathcal{P}) \\
 \text{s.t.} & (1) \sim (5), \text{C1} \sim \text{C3}
 \end{aligned} \tag{31}$$

V. PROPOSED SOLUTION

In this section, we propose the MAMO solution to solve the problem. As shown in Fig. 2, the solution model consists of K distributed actors, a learner, and a replay buffer. The learner consists of four neural networks, i.e., a local policy

network, a local critic network, a target policy network, and a target critic network, and the parameters of the four networks for vehicles are denoted by $\theta_{\mathbf{S}}^{\mu}$, $\theta_{\mathbf{S}}^{\mathcal{Q}}$, $\theta_{\mathbf{S}}^{\mu'}$, and $\theta_{\mathbf{S}}^{\mathcal{Q}'}$, respectively. Similarly, the parameters of the four networks for the edge node are denoted by $\theta_{\mathbf{E}}^{\mu}$, $\theta_{\mathbf{E}}^{\mathcal{Q}}$, $\theta_{\mathbf{E}}^{\mu'}$ and $\theta_{\mathbf{E}}^{\mathcal{Q}'}$, respectively. The local policy and local critic network parameters are randomly initialized. The parameters of target policy and target critic networks are initialized as the corresponding local network. K distributed actors are launched to interact with the environment and perform the replay experience storing. Each actor consists of a local vehicle policy network and a local edge policy network, which are denoted by $\theta_{\mathbf{S},k}^{\mu}$ and $\theta_{\mathbf{E},k}^{\mu}$, respectively, replicated from the local policy network of the learner. In each actor, each vehicle and the edge node determine actions via the corresponding policy network. The replay buffer \mathcal{B} with a maximum size $|\mathcal{B}|$ is initialized to store replay experiences.

A. Multi-Agent Distributed Policy Execution

In MAMO, each vehicle and the edge node determine their actions via the local policy networks in a distributed way. The local observation of the system state in vehicle s at time t is represented by

$$\mathbf{o}_s^t = \{t, s, l_s^t, \mathbf{D}_s, \Phi_s, \mathbf{D}_e^t, \mathbf{D}_{\mathbf{V}_e^t}, \mathbf{w}^t\} \tag{32}$$

where t is the time slot index; s is the vehicle index; l_s^t is the location of vehicle s ; \mathbf{D}_s represents the set of information that can be sensed by vehicle s ; Φ_s represents the sensing cost of information in \mathbf{D}_s ; \mathbf{D}_e^t represents the set of cached information in edge node e at time t ; $\mathbf{D}_{\mathbf{V}_e^t}$ represents the set of information required by DT-VEC in edge node e at time t , and \mathbf{w}^t represents the weight vector for each objective, which is randomly generated in each iteration. $\mathbf{w}^t = [w^{(1),t} \quad w^{(2),t}]$, where $w^{(1),t}$ denotes the weight of system quality, $w^{(2),t}$ denotes the weight of the system profit. And we have $w^{(j),t} \in$

$(0, 1), \forall j \in \{1, 2\}$, and $\sum_{j \in \{1, 2\}} w^{(j), t} = 1$. The local observation of the system state in edge node e at time t is represented by

$$\mathbf{o}_e^t = \{t, e, \mathbf{Dis}_{\mathbf{S}, e}^t, \mathbf{D}_1, \dots, \mathbf{D}_s, \dots, \mathbf{D}_S, \mathbf{D}_e^t, \mathbf{D}_{\mathbf{V}_e^t}, \mathbf{w}^t\} \quad (33)$$

where e is the edge node index, and $\mathbf{Dis}_{\mathbf{S}, e}^t$ represents the set of distances between vehicles and edge node e . Therefore, the system state at time t can be represented by $\mathbf{o}^t = \mathbf{o}_e^t \cup \mathbf{o}_1^t \cup \dots \cup \mathbf{o}_s^t \cup \dots \cup \mathbf{o}_S^t$.

The actions of vehicles are generated by the local vehicle policy network based on their local observations of the system state.

$$\mathbf{a}_s^t = \mu_{\mathbf{S}}(\mathbf{o}_s^t | \theta_{\mathbf{S}}^\mu) + \epsilon_s \mathcal{N}_s^t \quad (34)$$

where \mathcal{N}_s^t is an exploration noise to increase the diversity of vehicle actions, and ϵ_s is an exploration constant for vehicle s . The action space of vehicle s is represented by $\{\mathbf{C}_s^t, \{\lambda_{d,s}^t, p_{d,s}^t | \forall d \in \mathbf{D}_s^t\}, \pi_s^t\}$, where \mathbf{C}_s^t is the sensing information decision; $\lambda_{d,s}^t$ and $p_{d,s}^t$ are the sensing frequency and uploading priority of information $d \in \mathbf{D}_s^t$, respectively, and π_s^t is the transmission power of vehicle s at time t . The set of vehicle actions is denoted by $\mathbf{a}_{\mathbf{S}}^t = \{\mathbf{a}_s^t | \forall s \in \mathbf{S}\}$.

Then, the action of the edge node e can be obtained by the local edge policy network based on the system state as well as the actions of vehicles.

$$\mathbf{a}_e^t = \mu_{\mathbf{E}}(\mathbf{o}_e^t, \mathbf{a}_{\mathbf{S}}^t | \theta_{\mathbf{E}}^\mu) + \epsilon_e \mathcal{N}_e^t \quad (35)$$

where \mathcal{N}_e^t and ϵ_e are the exploration noise and exploration constant for the edge node e , respectively. The action space of edge node e is denoted by $\{b_{s,e}^t | \forall s \in \mathbf{S}_e^t\}$, where $b_{s,e}^t$ is the V2I bandwidth allocated by edge node e for vehicle s at time t . The joint action of vehicles and the edge node is denoted by $\mathbf{a}^t = \{\mathbf{a}_e^t, \mathbf{a}_1^t, \dots, \mathbf{a}_s^t, \dots, \mathbf{a}_S^t\}$.

The environment obtains the system reward vector by executing the joint action, which is represented by

$$\mathbf{r}^t = [r^{(1)}(\mathbf{a}_{\mathbf{S}}, \mathbf{a}_e^t | \mathbf{o}^t) \quad r^{(2)}(\mathbf{a}_{\mathbf{S}}, \mathbf{a}_e^t | \mathbf{o}^t)]^T \quad (36)$$

where $r^{(1)}(\mathbf{a}_{\mathbf{S}}, \mathbf{a}_e^t | \mathbf{o}^t)$ and $r^{(2)}(\mathbf{a}_{\mathbf{S}}, \mathbf{a}_e^t | \mathbf{o}^t)$ are the reward of two objectives (i.e., system quality and system profit), respectively, which can be computed by

$$\begin{cases} r^{(1)}(\mathbf{a}_{\mathbf{S}}, \mathbf{a}_e^t | \mathbf{o}^t) = 1/|\mathbf{V}_e^t| \sum_{\forall v \in \mathbf{V}_e^t} (1 - \text{QDT}_v) \\ r^{(2)}(\mathbf{a}_{\mathbf{S}}, \mathbf{a}_e^t | \mathbf{o}^t) = 1/|\mathbf{V}_e^t| \sum_{\forall v \in \mathbf{V}_e^t} (1 - \text{CDT}_v) \end{cases} \quad (37)$$

Accordingly, the reward of vehicle s in the j -th objective is obtained by the difference reward (DR) [33] based reward assignment, which is the difference between the system reward and the reward achieved without its action and can be represented by

$$r_s^{(j), t} = r^{(j)}(\mathbf{a}_{\mathbf{S}}, \mathbf{a}_e^t | \mathbf{o}^t) - r^{(j)}(\mathbf{a}_{\mathbf{S}-s}, \mathbf{a}_e^t | \mathbf{o}^t), \forall j \in \{1, 2\} \quad (38)$$

where $r^{(j)}(\mathbf{a}_{\mathbf{S}-s}, \mathbf{a}_e^t | \mathbf{o}^t)$ is the system reward achieved without the contribution of vehicle s , and it can be obtained by setting null action set for vehicle s . The reward vector of vehicle s at time t is denoted by \mathbf{r}_s^t and represented by $\mathbf{r}_s^t = [r_s^{(1), t} \quad r_s^{(2), t}]^T$. The set of the difference reward for vehicles is denoted by $\mathbf{r}_{\mathbf{S}}^t = \{\mathbf{r}_s^t | \forall s \in \mathbf{S}\}$.

On the other hand, the system reward is further transformed into a normalized reward for the edge node via min-max normalization. The reward of edge node e in the j -th objective at time t is computed by

$$r_e^{(j), t} = \frac{r^{(j)}(\mathbf{a}_{\mathbf{S}}, \mathbf{a}_e^t | \mathbf{o}^t) - \min_{\forall \mathbf{a}_e^{t'}} r^{(j)}(\mathbf{a}_{\mathbf{S}}, \mathbf{a}_e^{t'} | \mathbf{o}^t)}{\max_{\forall \mathbf{a}_e^{t'}} r^{(j)}(\mathbf{a}_{\mathbf{S}}, \mathbf{a}_e^{t'} | \mathbf{o}^t) - \min_{\forall \mathbf{a}_e^{t'}} r^{(j)}(\mathbf{a}_{\mathbf{S}}, \mathbf{a}_e^{t'} | \mathbf{o}^t)} \quad (39)$$

where $\min_{\forall \mathbf{a}_e^{t'}} r^{(j)}(\mathbf{a}_{\mathbf{S}}, \mathbf{a}_e^{t'} | \mathbf{o}^t)$ and $\max_{\forall \mathbf{a}_e^{t'}} r^{(j)}(\mathbf{a}_{\mathbf{S}}, \mathbf{a}_e^{t'} | \mathbf{o}^t)$ denotes the minimum and maximum of the system reward achieved with the unchanged vehicle actions $\mathbf{a}_{\mathbf{S}}^t$ under the same system state \mathbf{o}^t , respectively. The reward vector of edge node e at time t is denoted by \mathbf{r}_e^t , and represented by $\mathbf{r}_e^t = [r_e^{(1), t} \quad r_e^{(2), t}]^T$. The interaction experiences including the system state \mathbf{o}^t , vehicle actions $\mathbf{a}_{\mathbf{S}}^t$, edge action \mathbf{a}_e^t , vehicle rewards $\mathbf{r}_{\mathbf{S}}^t$, edge reward \mathbf{r}_e^t , weights \mathbf{w}^t , and next system state \mathbf{o}^{t+1} , are stored into the replay buffer \mathcal{B} . The interaction will continue until the training process of the learner is completed.

B. Multi-Objective Policy Evaluation

In this section, we propose the dueling critic network (DCN) to output the Q value by evaluating the advantage of the action over the average of random actions. There are two fully-connected networks, namely, the action-advantage (AA) network and the state-value (SV) network in the DCN. Note that the parameter of AA network for vehicles and the edge node are denoted by $\theta_{\mathbf{S}}^{\mathcal{A}}$ and $\theta_{\mathbf{E}}^{\mathcal{A}}$, respectively. Similarly, the parameter of the SV network for vehicles and the edge node are denoted by $\theta_{\mathbf{S}}^{\mathcal{V}}$ and $\theta_{\mathbf{E}}^{\mathcal{V}}$, respectively. The AA and SV networks estimate the advantage and value functions separately and produce a single output Q function via an aggregating module.

We denote the output scalar of AA network with the input of vehicle s by $A_{\mathbf{S}}(o_s^m, a_s^m, \mathbf{a}_{\mathbf{S}-s}^m, \mathbf{w}^m | \theta_{\mathbf{S}}^{\mathcal{A}})$, where $\mathbf{a}_{\mathbf{S}-s}^m$ denotes the action of other vehicles. Similarly, the output scalar of AA network with the input of edge node e is denoted by $A_{\mathbf{E}}(o_e^m, a_e^m, \mathbf{a}_{\mathbf{S}}^m, \mathbf{w}^m | \theta_{\mathbf{E}}^{\mathcal{A}})$, where $\mathbf{a}_{\mathbf{S}}^m$ denotes the action of all vehicles. The output scalar of SV network of vehicle s is denoted by $V(o_s^m, \mathbf{w}^m | \theta_{\mathbf{S}}^{\mathcal{V}})$. Similarly, the output scalar of SV network of edge node e is denoted by $V(o_e^m, \mathbf{w}^m | \theta_{\mathbf{E}}^{\mathcal{V}})$. Then, N actions are randomly generated and replaced with the agent action in the AA network to evaluate the average action value of random actions. We denote the n -th random action of vehicle s and edge node e by $a_s^{m, n}$ and $a_e^{m, n}$, respectively. Therefore, the advantage of the n -th random action of vehicle s and edge node e can be represented by $A_{\mathbf{S}}(o_s^m, a_s^{m, n}, \mathbf{a}_{\mathbf{S}-s}^m, \mathbf{w}^m | \theta_{\mathbf{S}}^{\mathcal{A}})$ and $A_{\mathbf{E}}(o_e^m, a_e^{m, n}, \mathbf{a}_{\mathbf{S}}^m, \mathbf{w}^m | \theta_{\mathbf{E}}^{\mathcal{A}})$, respectively.

The aggregating module of the Q function is constructed by evaluating the advantage of the agent action over the average advantage of random actions. Thus, the action values

of vehicle $s \in \mathbf{S}$ and edge node e are computed by

$$\begin{aligned} & Q_{\mathbf{S}} \left(o_s^m, a_s^m, \mathbf{a}_{\mathbf{S}-s}^m, \mathbf{w}^m \mid \theta_{\mathbf{S}}^Q \right) \\ &= V \left(o_s^m, \mathbf{w}^m \mid \theta_{\mathbf{S}}^V \right) + A_{\mathbf{S}} \left(o_s^m, a_s^m, \mathbf{a}_{\mathbf{S}-s}^m, \mathbf{w}^m \mid \theta_{\mathbf{S}}^A \right) \\ &- \frac{1}{N} \sum_{\forall n} A_{\mathbf{S}} \left(o_s^m, a_s^{m,n}, \mathbf{a}_{\mathbf{S}-s}^m, \mathbf{w}^m \mid \theta_{\mathbf{S}}^A \right) \end{aligned} \quad (40)$$

$$\begin{aligned} & Q_{\mathbf{E}} \left(o_e^m, a_e^m, \mathbf{a}_{\mathbf{S}}^m, \mathbf{w}^m \mid \theta_{\mathbf{E}}^Q \right) \\ &= V \left(o_e^m, \mathbf{w}^m \mid \theta_{\mathbf{E}}^V \right) + A_{\mathbf{E}} \left(o_e^m, a_e^m, \mathbf{a}_{\mathbf{S}}^m, \mathbf{w}^m \mid \theta_{\mathbf{E}}^A \right) \\ &- \frac{1}{N} \sum_{\forall n} A_{\mathbf{E}} \left(o_e^m, a_e^{m,n}, \mathbf{a}_{\mathbf{S}}^m, \mathbf{w}^m \mid \theta_{\mathbf{E}}^A \right) \end{aligned} \quad (41)$$

where $\theta_{\mathbf{S}}^Q$ and $\theta_{\mathbf{S}}^Q$ contain the parameters of the corresponding AA and SV networks.

$$\begin{aligned} \theta_{\mathbf{S}}^Q &= (\theta_{\mathbf{S}}^A, \theta_{\mathbf{S}}^V), \theta_{\mathbf{S}}^{Q'} = (\theta_{\mathbf{S}}^{A'}, \theta_{\mathbf{S}}^{V'}) \\ \theta_{\mathbf{E}}^Q &= (\theta_{\mathbf{E}}^A, \theta_{\mathbf{E}}^V), \theta_{\mathbf{E}}^{Q'} = (\theta_{\mathbf{E}}^{A'}, \theta_{\mathbf{E}}^{V'}) \end{aligned} \quad (42)$$

C. Policy and Critic Network Learning and Updating

A minibatch of M transitions is sampled from the replay buffer \mathcal{B} to train the policy and critic networks of vehicles and the edge node, which is denoted by $(o_{\mathbf{S}}^m, o_e^m, \mathbf{w}^m, \mathbf{a}_{\mathbf{S}}^m, a_e^m, \mathbf{r}_{\mathbf{S}}^m, \mathbf{r}_e^m, o_{\mathbf{S}}^{m+1}, o_e^{m+1}, \mathbf{w}^{m+1})$. The target value of vehicle s is denoted by

$$y_s^m = \mathbf{r}_s^m \mathbf{w}^m + \gamma Q'_{\mathbf{S}} \left(o_s^{m+1}, a_s^{m+1}, \mathbf{a}_{\mathbf{S}-s}^{m+1}, \mathbf{w}^{m+1} \mid \theta_{\mathbf{S}}^{Q'} \right) \quad (43)$$

where $Q'_{\mathbf{S}}(o_s^{m+1}, a_s^{m+1}, \mathbf{a}_{\mathbf{S}-s}^{m+1}, \mathbf{w}^{m+1} \mid \theta_{\mathbf{S}}^{Q'})$ denotes the action value generated by the target vehicle critic network; γ is the discount; $\mathbf{a}_{\mathbf{S}-s}^{m+1}$ is the next vehicle actions without the vehicle s , i.e., $\mathbf{a}_{\mathbf{S}-s}^{m+1} = \{a_1^{m+1}, \dots, a_{s-1}^{m+1}, a_{s+1}^{m+1}, \dots, a_S^{m+1}\}$, and a_s^{m+1} is the next action of vehicle s generated by the target vehicle policy network based on its local observation of next system state, i.e., $a_s^{m+1} = \mu'_{\mathbf{S}}(o_s^{m+1} \mid \theta_{\mathbf{S}}^{Q'})$. Similarly, the target value of edge node e is denoted by

$$y_e^m = \mathbf{r}_e^m \mathbf{w}^m + \gamma Q'_{\mathbf{E}} \left(o_e^{m+1}, a_e^{m+1}, \mathbf{a}_{\mathbf{S}}^{m+1}, \mathbf{w}^{m+1} \mid \theta_{\mathbf{E}}^{Q'} \right) \quad (44)$$

where $Q'_{\mathbf{E}}(o_e^{m+1}, a_e^{m+1}, \mathbf{a}_{\mathbf{S}}^{m+1}, \mathbf{w}^{m+1} \mid \theta_{\mathbf{E}}^{Q'})$ denotes the action value generated by the target edge critic network; $\mathbf{a}_{\mathbf{S}}^{m+1}$ is the next vehicle actions, and a_e^{m+1} denotes the next edge action, which can be obtained by the target edge policy network based on its local observation of the next system state, i.e., $a_e^{m+1} = \mu'_{\mathbf{E}}(o_e^{m+1}, \mathbf{a}_{\mathbf{S}}^{m+1} \mid \theta_{\mathbf{E}}^{Q'})$.

The loss function of the vehicle critic network and edge critic network are obtained by the categorical distribution temporal difference (TD) learning, which is represented by

$$\mathcal{L} \left(\theta_{\mathbf{S}}^Q \right) = \frac{1}{M} \sum_m \frac{1}{S} \sum_s Y_s^m \quad (45)$$

$$\mathcal{L} \left(\theta_{\mathbf{E}}^Q \right) = \frac{1}{M} \sum_m Y_e^m \quad (46)$$

where Y_s^m and Y_e^m are the squares of the difference between the target value and the action value generated by the local critic network for vehicle s and edge node e , respectively.

$$Y_s^m = \left(y_s^m - Q_{\mathbf{S}} \left(o_s^m, a_s^m, \mathbf{a}_{\mathbf{S}-s}^m, \mathbf{w}^m \mid \theta_{\mathbf{S}}^Q \right) \right)^2 \quad (47)$$

$$Y_e^m = \left(y_e^m - Q_{\mathbf{E}} \left(o_e^m, a_e^m, \mathbf{a}_{\mathbf{S}}^m, \mathbf{w}^m \mid \theta_{\mathbf{E}}^Q \right) \right)^2 \quad (48)$$

The vehicle and edge policy network parameters are updated via deterministic policy gradient.

$$\nabla_{\theta_{\mathbf{S}}^{\mu}} \mathcal{J}(\theta_{\mathbf{S}}^{\mu}) \approx \frac{1}{M} \sum_m \frac{1}{S} \sum_s P_s^m \quad (49)$$

$$\nabla_{\theta_{\mathbf{E}}^{\mu}} \mathcal{J}(\theta_{\mathbf{E}}^{\mu}) \approx \frac{1}{M} \sum_m P_e^m \quad (50)$$

where

$$P_s^m = \nabla_{a_s^m} Q_{\mathbf{S}} \left(o_s^m, a_s^m, \mathbf{a}_{\mathbf{S}-s}^m, \mathbf{w}^m \mid \theta_{\mathbf{S}}^Q \right) \nabla_{\theta_{\mathbf{S}}^{\mu}} \mu_{\mathbf{S}} \left(o_s^m \mid \theta_{\mathbf{S}}^{\mu} \right) \quad (51)$$

$$P_e^m = \nabla_{a_e^m} Q_{\mathbf{E}} \left(o_e^m, a_e^m, \mathbf{a}_{\mathbf{S}}^m, \mathbf{w}^m \mid \theta_{\mathbf{E}}^Q \right) \nabla_{\theta_{\mathbf{E}}^{\mu}} \mu_{\mathbf{E}} \left(o_e^m, \mathbf{a}_{\mathbf{S}}^m \mid \theta_{\mathbf{E}}^{\mu} \right) \quad (52)$$

The local policy and critic network parameters are updated with the learning rate α and β . Vehicles and the edge node update the parameters of target networks periodically, i.e., when $t \bmod t_{\text{tgt}} = 0$, where t_{tgt} is the parameter updating period of the target networks,

$$\begin{aligned} \theta_{\mathbf{S}}^{\mu'} &\leftarrow n_{\mathbf{S}} \theta_{\mathbf{S}}^{\mu} + (1 - n_{\mathbf{S}}) \theta_{\mathbf{S}}^{\mu'}, \theta_{\mathbf{S}}^{Q'} \leftarrow n_{\mathbf{S}} \theta_{\mathbf{S}}^Q + (1 - n_{\mathbf{S}}) \theta_{\mathbf{S}}^{Q'} \\ \theta_{\mathbf{E}}^{\mu'} &\leftarrow n_{\mathbf{E}} \theta_{\mathbf{E}}^{\mu} + (1 - n_{\mathbf{E}}) \theta_{\mathbf{E}}^{\mu'}, \theta_{\mathbf{E}}^{Q'} \leftarrow n_{\mathbf{E}} \theta_{\mathbf{E}}^Q + (1 - n_{\mathbf{E}}) \theta_{\mathbf{E}}^{Q'} \end{aligned} \quad (53)$$

with $n_{\mathbf{S}} \ll 1$ and $n_{\mathbf{E}} \ll 1$. The network parameters of policy networks at the distributed actors are also updated periodically, i.e., when $t \bmod t_{\text{act}} = 0$, where t_{act} is the parameter updating period of the policy network at the distributed actors.

$$\begin{aligned} \theta_{\mathbf{S},k}^{\mu} &\leftarrow \theta_{\mathbf{S}}^{\mu'}, \theta_{\mathbf{S},k}^Q \leftarrow \theta_{\mathbf{S}}^{Q'}, \forall k \in \{1, 2, \dots, K\} \\ \theta_{\mathbf{E},k}^{\mu} &\leftarrow \theta_{\mathbf{E}}^{\mu'}, \theta_{\mathbf{E},k}^Q \leftarrow \theta_{\mathbf{E}}^{Q'}, \forall k \in \{1, 2, \dots, K\} \end{aligned} \quad (54)$$

VI. PERFORMANCE EVALUATION

A. Experiment Setup

In this section, we use Python 3.9.13 and TensorFlow 2.8.0 to evaluate the performance of the proposed MAMO scheme using a Ubuntu 20.04 server with an AMD Ryzen 9 5950X 16-core processor @ 3.4 GHz, two NVIDIA GeForce RTX 3090 GPUs, and 64 GB memory. We consider the general scenario in a 1×1 km² square area, where the realistic vehicular trajectories are utilized as traffic inputs collected from Didi GAIA open data set [34]. On the basis of referring to [32] and [35], the simulation parameter settings are as follows. The V2I communication range is set as 500 m. The transmission power is set as 100 mW. The AWGN and reliability threshold are set as -90 dBm and 0.9, respectively. The channel fading gains of V2I communications follow the Gaussian distribution with a mean of 2 and a variance of 0.4. The weighting factors for Θ_v , Ψ_v , Ξ_v , Φ_v , and Ω_v are set as 0.6, 0.4, 0.2, 0.4, and 0.4, respectively.

For the implementation of the proposed solution, the architectures and hyperparameters of the policy and critic networks are described as follows. The local policy network is a four-layer fully connected neural network with two hidden layers, where the numbers of neurons are 256 and 128, respectively. The architecture of the target policy network is the same as the local policy network. The local critic network is a four-layer fully connected neural network with two hidden layers, where

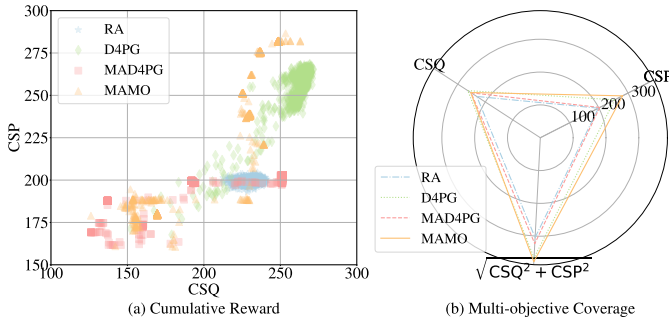


Fig. 3. Convergence comparison

the numbers of neurons are 512 and 256, respectively. The architecture of the target critic network is the same as the local critic network. The discount, batch size, and maximum replay buffer size are set to 0.996, 256, and 1×10^6 , respectively. The learning rates for policy and critic networks are set to 1×10^{-4} and 1×10^{-4} , respectively.

Three comparable algorithms are implemented as follows.

- *Random Allocation (RA)*: it randomly selects one action to determine the sensing information, sensing frequencies, uploading priorities, transmission power, and V2I bandwidth allocation.
- *Distributed Distributional Deep Deterministic Policy Gradient (D4PG)* [36]: it implements an agent at the edge node to determine the sensing information, sensing frequencies, uploading priorities, transmission power, and V2I bandwidth allocation in a centralized way based on the system state. The system quality and the system profit weights are set as 0.5 and 0.5, respectively.
- *Multi-Agent Distributed Distributional Deep Deterministic Policy Gradient (MAD4PG)*: it is a multi-agent version of D4PG, which is implemented in vehicles to decide the sensing information, sensing frequencies, uploading priorities, and transmission power based on local observation of the physical environment, and the edge node to determine the V2I bandwidth allocation. The system quality and the system profit weights are set as 0.5 and 0.5, respectively.

For performance evaluation, four primary metrics named *Cumulative system quality (CSQ)*, *Cumulative System Profit (CSP)*, *Average Quality of Digital Twin (AQDT)*, and *Average Cost of Digital Twin (ACDT)* are obtained based on Eqs. 26, 30, 19, and 25, respectively. We further design the five metrics named *Average Timeliness (AT)*, *Average Consistency (AC)*, *Average Redundancy (AR)*, *Average Sensing Cost (ASC)*, and *Average Transmission Cost (ATC)* based on Eqs. 17, 18, 21, 22, and 24, respectively.

B. Result Analysis

1) *Algorithm convergence*: Figure 3 compares the convergence of the four algorithms. In particular, Fig. 3(a) compares the CSQ and CSP of the four algorithms. As noted, MAMO achieves the highest CSP (around 281), and the CSQ of MAMO is just next to D4PG (around 253), indicating that MAMO can achieve a tradeoff between system quality and

system cost, i.e., maximize the system quality at the lowest cost. As a comparison, D4PG achieves a CSP of around 254 and a CSQ of around 263, while MAD4PG achieves a CSP of around 203 and a CSQ of around 251. And RA achieves a CSP of around 198 and a CSQ of around 230. It can be further verified in Fig. 3(b), which compares the multi-objective coverage of the four algorithms. MAMO achieves the maximum multi-objective coverage. Meanwhile, MAMO and D4PG are similar in terms of multi-objective coverage. The reason is that D4PG can obtain such performance due to centralized scheduling and global observation of the system state. However, it is realistic for MAMO to achieve in a distributed manner with the local observation of the system state.

2) *Effect of traffic scenarios*: Figure 4 compare the performance of the four algorithms under different traffic scenarios, in which the realistic vehicular trajectories are extracted from different time and spaces, i.e., 1): a 1 km \times 1 km area of Qingyang District, Chengdu, China, from 8:00 to 8:05, on 16 Nov. 2016; 2): the same area from 23:00 to 23:05, on 16 Nov. 2016; 3): a 1 km \times 1 km area of Beilin District, Xian, China, from 8:00 to 8:05, on 27 Nov. 2016. Figure 4(a) compares the CSQ and CSP of the four algorithms. As demonstrated, MAMO achieves a tradeoff between the system quality and system cost in all scenarios, which is very close to the centralized approach, i.e., the D4PG algorithm, with an average performance difference of around 1.5 %. It is noted that MAMO achieves the average reward of about 9.0 % and 7.2 % over RA and MAD4PG under multi-objectives, respectively. Figure 4(b) shows the AQDT and ACDT of the four algorithms. It is expected that MAMO achieves the lowest ACDT under all the scenarios. As noted, the ACDT of MAD4PG and RA are similar under different traffic scenarios. The reason is that the same reward cannot evaluate the actions of different agents, which does not encourage distributed agents to cooperate with each other. Figure 4(c) compares the composition of AQDT of the four algorithms under different traffic scenarios, which breaks down the AQDT into two parts and demonstrates the proportion of AT and AC, respectively. As noted, the AT of MAMO is lower than RA and MAD4PG under different scenarios. However, the AC of MAMO is higher than that of RA and MAD4PG. This is mainly because the weights of timeliness and consistency in QDT make timeliness more important for MAMO. Figure 4(d) compares the composition of ACDT of the four algorithms, which breaks down the ACDT into three parts and demonstrates the proportion of AR, ASC, and ATC, respectively. As noted, the AR of MAMO is the lowest under different scenarios, especially the AR of the MAMO is 0. It demonstrates that the MAMO can cooperate among vehicles by sensing information cooperatively, thus minimizing information redundancy. Meanwhile, the ASC and ATC of MAMO are the lowest under different traffic scenarios, which indicates that MAMO achieves the lowest cost in constructing the views.

3) *Effect of edge bandwidths*: Figure 5 compares the performance of the four algorithms under different bandwidths of the edge node. In this set of experiments, we consider the bandwidth of edge nodes increases from 1 MHz to 3 MHz.

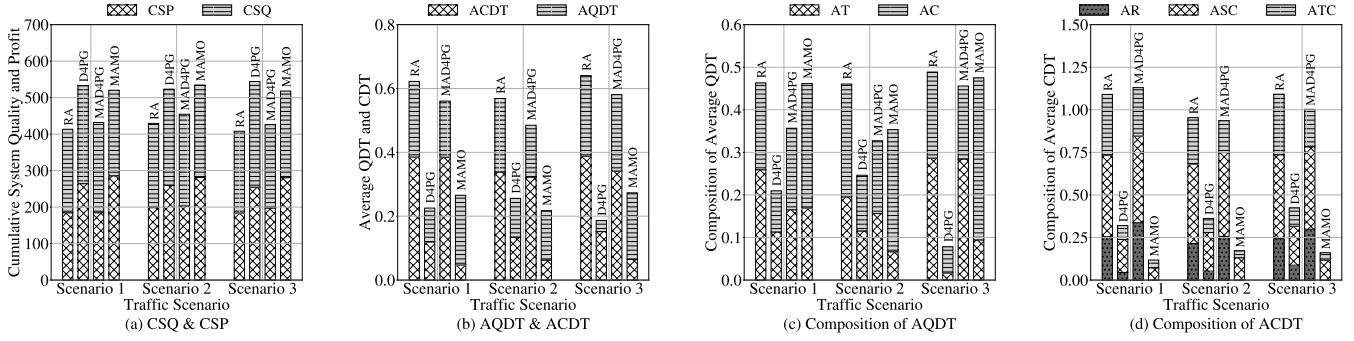


Fig. 4. Performance comparison under different traffic scenarios

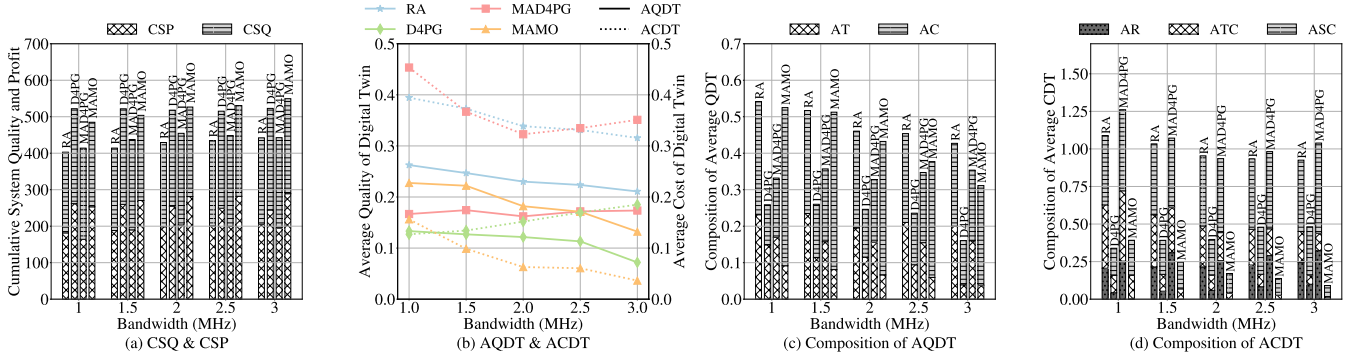


Fig. 5. Performance comparison under different bandwidths of the edge node

A larger bandwidth represents that the allocated bandwidth for each vehicle can be enlarged, which results in a shorter information uploading time. Figure 5(a) compares the CSQ and CSP of the four algorithms. As the bandwidth increases, the sum of the CSQ and CSP of all algorithms increases accordingly. Meanwhile, note that the improvement in the sum of the CSQ and CSP is greater for MAMO than for RA, D4PG, and MAD4PG when the bandwidth increases. This is because the cooperation of sensing and uploading information among vehicles is more efficient in MAMO with rich bandwidth. The advantage can be further justified by Fig. 5(b), which shows the AQDT and ACDT of the four algorithms. In particular, MAMO is the only solution whose AQDT and ACDT decrease when the bandwidth increases, except for RA. That shows that the MAMO can optimize the two conflicting objectives simultaneously. Figure 5(c) compares the AT and AC of the four algorithms under different edge bandwidths. MAMO achieves better performance than the other three algorithms in terms of AT. It is noted that the AT and AC of the four algorithms are similar when the bandwidth increases from 1 MHz to 1.5 MHz. This is because improving the timeliness and consistency of views with limited bandwidth is more challenging. Figure 5(d) compares the AR, ATC, and ASC of the four algorithms. MAMO is expected to achieve the lowest AR, demonstrating MAMO’s superiority in reducing redundant sensing and uploading by cooperation between vehicles. It is observed that the ATC of the four algorithms decreases when the bandwidth increases. The reason is that when the bandwidth increases, the information uploading time

decreases, resulting in a lower transmission cost. As expected, the ASC and ATC of MAMO remain at the lowest level in most cases.

4) *Effect of average information number of DT-VEC*: Figure 6 compares the performance of the four algorithms under different information requirements of DT-VEC, in which the average number of information required by DT-VEC increases from 3 to 7. A larger average number of the required information of DT-VEC indicates that the vehicles have more significant sensing and uploading workloads, which leads to worse-quality DT-VEC. Figure 6(a) compares the CSQ and CSP of the four algorithms. With the increasing average required information number, the sum of CSQ and CSP of the four algorithms decreases accordingly. As noted, the MAMO keeps the highest sum of CSQ and CSP in all cases. Figure 6(b) compares the AQDT and ACDT of the four algorithms. As expected, when the average information number increases, the AQDT and ACDT of the four algorithms increase accordingly. The reason is that the vehicles may sense and upload more information to meet the requirement of DT-VEC under the same limited resource constraints. Figure 6(c) compares the AT and AC of the four algorithms. As expected, MAMO achieves the best performance in terms of AT. It is observed that the performance gap between MAMO, MAD4PG, and D4PG is small when the average information number is small (i.e., around 3). The reason is the scheduling effect is not significant when there are sufficient resources. Figure 6(d) compares the AR, ATC, and ASC of the four algorithms. MAMO can remain the lowest ASC and ATC across all cases. It is also noted that

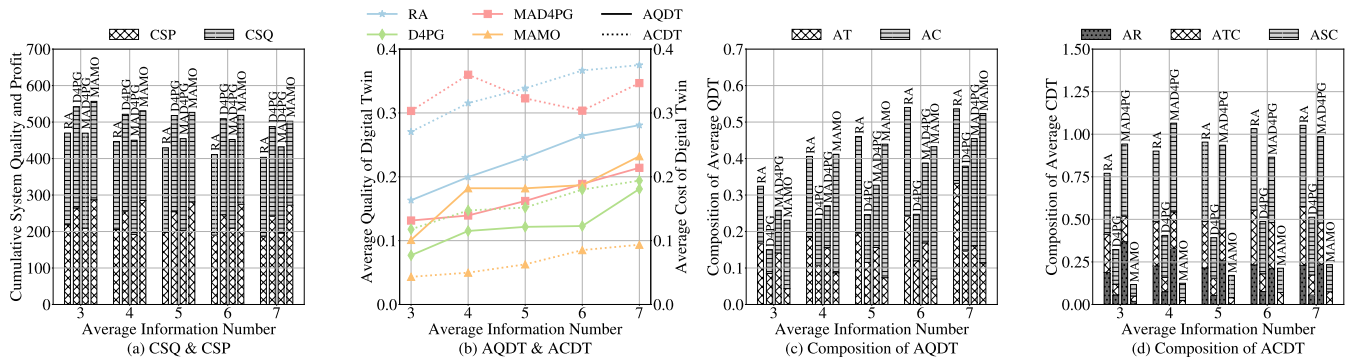


Fig. 6. Performance comparison under different information requirements on DT-VEC

the ASC and ATC of the four algorithms increase when the average information number increases. The reason is that the average amount of information required by DT-VEC increases, resulting in higher vehicle sensing and transmission costs.

VII. CONCLUSION

In this paper, the DT-VEC architecture was presented, in which heterogeneous information is sensed via ISAC and onboard sensors and uploaded via V2I communications. The sensed information is fused and modeled into DT-VEC, forming logical views in edge nodes to reflect the physical vehicular environment. In particular, the DT-VEC model was derived by giving the formal definition. The ISAC-assisted sensing model was derived based on multi-class M/G/1 priority queue, and the reliability-guaranteed uploading model was derived based on channel fading distribution and SNR threshold. On this basis, two metrics, QDT and CDT, were designed to evaluate the quality and cost of the DT-VEC at the edge nodes. Then, the system quality and system cost were modeled, and the bi-objective problem was formulated to maximize the system quality and minimize the system cost, simultaneously. Further, the MAMO solution was proposed and implemented distributedly in the vehicles and the edge nodes. In particular, a dueling critic network was adopted to output action value by evaluating the advantage of action over the average of random actions. Finally, the performance evaluation was given, which demonstrates the superiority of the proposed solution.

REFERENCES

- [1] H. Zhu, K.-V. Yuen, L. Mihaylova, and H. Leung, "Overview of environment perception for intelligent vehicles," *IEEE Trans. Intell. Transp. Syst.*, vol. 18, no. 10, pp. 2584–2601, 2017.
- [2] A. Liu, Z. Huang, M. Li, Y. Wan, W. Li, T. X. Han, C. Liu, R. Du, D. K. P. Tan, J. Lu, Y. Shen, F. Colone, and K. Chetty, "A survey on fundamental limits of integrated sensing and communication," *IEEE Commun. Surv. Tutor.*, vol. 24, no. 2, pp. 994–1034, 2022.
- [3] M. M. Saad, M. T. R. Khan, S. H. A. Shah, and D. Kim, "Advancements in vehicular communication technologies: C-v2x and nr-v2x comparison," *IEEE Commun. Mag.*, vol. 59, no. 8, pp. 107–113, 2021.
- [4] P. Dai, F. Song, K. Liu, Y. Dai, P. Zhou, and S. Guo, "Edge intelligence for adaptive multimedia streaming in heterogeneous internet of vehicles," *IEEE Trans. Mob. Comput.*, 2021, doi: 10.1109/TMC.2021.3106147.
- [5] H. X. Nguyen, R. Trestian, D. To, and M. Tatipamula, "Digital twin for 5g and beyond," *IEEE Commun. Mag.*, vol. 59, no. 2, pp. 10–15, 2021.
- [6] Y. Liu, M. Li, A. Liu, J. Lu, and T. X. Han, "Information-theoretic limits of integrated sensing and communication with correlated sensing and channel states for vehicular networks," *IEEE Trans. Veh. Technol.*, vol. 71, no. 9, pp. 10 161–10 166, 2022.

- [7] Q. Zhang, H. Sun, Z. Wei, and Z. Feng, "Sensing and communication integrated system for autonomous driving vehicles," in *Proc. IEEE Conf. on Comput. Commun. Workshops (INFOCOM WKSHPS)*. IEEE, 2020, pp. 1278–1279.
- [8] W. Yuan, Z. Wei, S. Li, J. Yuan, and D. W. K. Ng, "Integrated sensing and communication-assisted orthogonal time frequency space transmission for vehicular networks," *IEEE J. Sel. Top. Signal Process.*, vol. 15, no. 6, pp. 1515–1528, 2021.
- [9] K. Liu, K. Xiao, P. Dai, V. C. Lee, S. Guo, and J. Cao, "Fog computing empowered data dissemination in software defined heterogeneous vanets," *IEEE Trans. Mob. Comput.*, vol. 20, no. 11, pp. 3181–3193, 2021.
- [10] A. Singh, G. S. Aujla, and R. S. Bali, "Intent-based network for data dissemination in software-defined vehicular edge computing," *IEEE Trans. Intell. Transp. Syst.*, vol. 22, no. 8, pp. 5310–5318, 2020.
- [11] Y. Dai, D. Xu, K. Zhang, S. Maharjan, and Y. Zhang, "Deep reinforcement learning and permissioned blockchain for content caching in vehicular edge computing and networks," *IEEE Trans. Veh. Technol.*, vol. 69, no. 4, pp. 4312–4324, 2020.
- [12] K. Xiao, K. Liu, X. Xu, L. Feng, Z. Wu, and Q. Zhao, "Cooperative coding and caching scheduling via binary particle swarm optimization in software-defined vehicular networks," *Neural. Comput. Appl.*, vol. 33, no. 5, pp. 1467–1478, 2021.
- [13] Z. Su, Y. Hui, Q. Xu, T. Yang, J. Liu, and Y. Jia, "An edge caching scheme to distribute content in vehicular networks," *IEEE Trans. Veh. Technol.*, vol. 67, no. 6, pp. 5346–5356, 2018.
- [14] B. Shang, L. Liu, and Z. Tian, "Deep learning-assisted energy-efficient task offloading in vehicular edge computing systems," *IEEE Trans. Veh. Technol.*, vol. 70, no. 9, pp. 9619–9624, 2021.
- [15] C. Liu, K. Liu, H. Ren, X. Xu, R. Xie, and J. Cao, "Rtds: real-time distributed strategy for multi-period task offloading in vehicular edge computing environment," *Neural. Comput. Appl.*, 2021, doi: 10.1007/s00521-021-05766-5.
- [16] Z. Liu, P. Dai, H. Xing, Z. Yu, and W. Zhang, "A distributed algorithm for task offloading in vehicular networks with hybrid fog/cloud computing," *IEEE Trans. Syst., Man, Cybern.*, vol. 52, no. 7, pp. 4388–4401, 2022.
- [17] K. Liu, X. Xu, M. Chen, B. Liu, L. Wu, and V. C. Lee, "A hierarchical architecture for the future internet of vehicles," *IEEE Commun. Mag.*, vol. 57, no. 7, pp. 41–47, 2019.
- [18] S.-H. Wang, S.-C. Hsia, and M.-J. Zheng, "Deep learning-based raindrop quantity detection for real-time vehicle-safety application," *IEEE Trans. Consum. Electron.*, vol. 67, no. 4, pp. 266–274, 2021.
- [19] W.-J. Chang, L.-B. Chen, and Y.-Z. Chiou, "Design and implementation of a drowsiness-fatigue-detection system based on wearable smart glasses to increase road safety," *IEEE Trans. Consum. Electron.*, vol. 64, no. 4, pp. 461–469, 2018.
- [20] Y. Zhang, L. Chu, Y. Ou, C. Guo, Y. Liu, and X. Tang, "A cyber-physical system-based velocity-profile prediction method and case study of application in plug-in hybrid electric vehicle," *IEEE T. Cybern.*, vol. 51, no. 1, pp. 40–51, 2019.
- [21] T. Zhang, Y. Zou, X. Zhang, N. Guo, and W. Wang, "Data-driven based cruise control of connected and automated vehicles under cyber-physical system framework," *IEEE Trans. Intell. Transp. Syst.*, vol. 22, no. 10, pp. 6307–6319, 2020.
- [22] C. Li, H. Zhang, T. Zhang, J. Rao, L. Y. Wang, and G. Yin, "Cyber-physical scheduling for predictable reliability of inter-vehicle commu-

nications,” *IEEE Trans. Veh. Technol.*, vol. 69, no. 4, pp. 4192–4206, 2020.

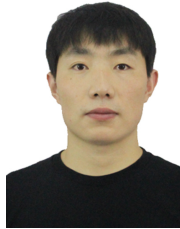
- [23] Y. Lian, Q. Yang, W. Xie, and L. Zhang, “Cyber-physical system-based heuristic planning and scheduling method for multiple automatic guided vehicles in logistics systems,” *IEEE Trans. Ind. Inform.*, vol. 17, no. 11, pp. 7882–7893, 2021.
- [24] C. Lv, X. Hu, A. Sangiovanni-Vincentelli, Y. Li, C. M. Martinez, and D. Cao, “Driving-style-based codesign optimization of an automated electric vehicle: A cyber-physical system approach,” *IEEE Trans. Ind. Electron.*, vol. 66, no. 4, pp. 2965–2975, 2018.
- [25] Y.-M. Wi, J.-U. Lee, and S.-K. Joo, “Electric vehicle charging method for smart homes/buildings with a photovoltaic system,” *IEEE Trans. Consum. Electron.*, vol. 59, no. 2, pp. 323–328, 2013.
- [26] K. Liu, V. C. S. Lee, J. K.-Y. Ng, J. Chen, and S. H. Son, “Temporal data dissemination in vehicular cyber-physical systems,” *IEEE Trans. Intell. Transp. Syst.*, vol. 15, no. 6, pp. 2419–2431, 2014.
- [27] P. Dai, K. Liu, L. Feng, H. Zhang, V. C. S. Lee, S. H. Son, and X. Wu, “Temporal information services in large-scale vehicular networks through evolutionary multi-objective optimization,” *IEEE Trans. Intell. Transp. Syst.*, vol. 20, no. 1, pp. 218–231, 2019.
- [28] S. T. Rager, E. N. Ciftcioglu, R. Ramanathan, T. F. La Porta, and R. Govindan, “Scalability and satisfiability of quality-of-information in wireless networks,” *IEEE-ACM Trans. Netw.*, vol. 26, no. 1, pp. 398–411, 2017.
- [29] D. D. Yoon, B. Ayalew, and G. G. M. N. Ali, “Performance of decentralized cooperative perception in v2v connected traffic,” *IEEE Trans. Intell. Transp. Syst.*, vol. 23, no. 7, pp. 6850–6863, 2022.
- [30] M. Moltafet, M. Leinonen, and M. Codreanu, “On the age of information in multi-source queueing models,” *IEEE Trans. Commun.*, vol. 68, no. 8, pp. 5003–5017, 2020.
- [31] T. Takine, “Queue length distribution in a fifo single-server queue with multiple arrival streams having different service time distributions,” *Queueing Syst.*, vol. 39, no. 4, pp. 349–375, 2001.
- [32] A. K. Sadek, Z. Han, and K. R. Liu, “Distributed relay-assignment protocols for coverage expansion in cooperative wireless networks,” *IEEE Trans. Mob. Comput.*, vol. 9, no. 4, pp. 505–515, 2009.
- [33] J. N. Foerster, G. Farquhar, T. Afouras, N. Nardelli, and S. Whiteson, “Counterfactual multi-agent policy gradients,” in *Proc. AAAI Conf. on Artif. Intell. (AAAI)*, 2018.
- [34] “Data source: Didi chuxing gaia open dataset initiative,” <https://outreach.didichuxing.com/research/opendata/en/>.
- [35] J. Wang, K. Liu, B. Li, T. Liu, R. Li, and Z. Han, “Delay-sensitive multi-period computation offloading with reliability guarantees in fog networks,” *IEEE Trans. Mob. Comput.*, vol. 19, no. 9, pp. 2062–2075, 2019.
- [36] G. Barth-Maron, M. W. Hoffman, D. Budden, W. Dabney, D. Horgan, D. TB, A. Muldal, N. Heess, and T. Lillicrap, “Distributed distributional deterministic policy gradients,” in *Proc. Int. Conf. Learn. Represent. (ICLR)*, 2018.



Kai Liu (Senior Member, IEEE) received the Ph.D. degree in computer science from the City University of Hong Kong in 2011. He is currently a Full Professor with the College of Computer Science, Chongqing University, China. From 2010 to 2011, he was a Visiting Scholar with the Department of Computer Science, University of Virginia, Charlottesville, VA, USA. From 2011 to 2014, he was a Postdoctoral Fellow with Nanyang Technological University, Singapore, City University of Hong Kong, and Hong Kong Baptist University, Hong Kong. His research interests include mobile computing, pervasive computing, intelligent transportation systems, and the Internet of Vehicles.



Penglin Dai (Member, IEEE) received the B.S. degree in mathematics and applied mathematics and the Ph.D. degree in computer science from Chongqing University, Chongqing, China, in 2012 and 2017, respectively. He is currently an Associate Professor with the School of Computing and Artificial Intelligence, Southwest Jiaotong University, Chengdu, China. His research interests include intelligent transportation systems and vehicular cyber-physical systems.



Biwen Chen received the Ph.D. degree from School of Computer, Wuhan University in 2020. He is currently an assistant professor of the School of Computer, Chongqing University. His main research interests include cryptography, information security and blockchain.



Xincao Xu received the B.S. degree in network engineering from the North University of China, Taiyuan, China, in 2017. He is currently pursuing the Ph.D. degree in computer science at Chongqing University, Chongqing, China. His research interests include vehicular networks, edge computing, and deep reinforcement learning.